A Dynamic Advisory Speed Limit Algorithm of Eco-Driving Strategies Based on Phase Time Control

Ximeng Fan

A thesis presented for the degree of
Civil and Environmental Engineering M.S. (CEE)
Samueli School of Engineering
University of California,Irvine

Committee Members:
Wenlong Jin (Chair), Associate Professor
R. Jayakrishnan, Professor
Will Recker, Distinguished Professor
Date: June, 2020

CONTENTS

LIST OF FIGURES

LIST OF TABLE

ACKNOWLEDGEMENTS

I would like to thank my advisor professor Jin in particular for his generous help, patient guidance and valuable suggestions on both methodology and writing. I also appreciate the help from professor Jay and professor Recker as committee members.

I want to thank my parents and grandparents for always supporting me to do what I love and regard my happiness as the most important thing. Thanks to my four best friends, Mengyuan & Zhou & Ziya & Lianghui, it is my great fortune to have this twelve-year-friendship. Thanks to Tong & Xiaolan and Chenyu, for their company and witnessing my growth. I also want to say thank you to my colleagues, Xuting & Lu & Dingtong & Yiqiao & Boyuan & Guoliang, etc., for making me feel that life in California is not alone.

Last but not least, I want to thank Huiyu Wang, four years of liking you was a period of time that filled me with motivation. Now that I will move on, and I wish you all the best in the future.

ABSTRACT OF THE THESIS

A Dynamic Advisory Speed Limit Algorithm of Eco-Driving Strategies Based on Phase Time Control

by

Ximeng Fan

June, 2020

University of California, Irvine

Degree title: Civil and Environmental Engineering M.S. (CEE), 2020 Spring

Professor Wenlong Jin, Chair

The concept of eco-driving is based on environmental factors such as fuel consumption. A large number of existing studies have proven the effectiveness of eco-driving in environmental protection. However, there still lacks a clear understanding of the impacts of eco-driving on overall performance of a signalized road network at different congestion levels. In this paper, we systematically study the impacts of a green driving strategy based on the advisory speed limit (ASL) to smooth the vehicle trajectories. We first analyze the limitations of the static ASL algorithm and propose the dynamic ASL algorithm based on it. We then review the car-following models, including Newell's car-following model, BA Newell's car-following and intelligent driver model (IDM), that we utilize for simulating vehicle movements. For evaluation, we introduce network fundamental diagrams (NFD) and fuel consumption as indicators to measure the efficiency of our algorithm. With numerical results, we demonstrate that our dynamic ASL can change the start-up and clearance behaviors so as to smooth vehicles' trajectories and improve system mobility. In particular, it mainly plays a role under saturated conditions; with proper car-following models, capacity can be increased by up to 40% and fuel consumption can be reduced by up to 25%. We further demonstrate that our algorithm is effective cooperatively for different market penetration rates (MPR) of connected vehicles and work out a proper range of the ASL implementation area. Our algorithm can make a contribution even when 5% of the vehicles adopt our algorithm, with a higher MPR, it can be increasingly more efficient; and the recommended ASL implementation area is in the range of 100 meters to 150 meters. In the future we are interested in extending our

idea for over-saturated conditions and some more complicated transportation systems.

Keywords: Eco-driving, Static advisory speed limit, Dynamic advisory speed limit, Network fundamental diagram, Newell's car-following model, Intelligent driver model, VT-micro model, Market penetration rate

Chapter 1

Introduction

According to a survey in 2011, "Americans wasted nearly 4.8 billion hours and 3.9 billion gallons of fuel sitting in traffic, at a cost of $115 billion—more than one-sixth the amount of oil imported annually from the Persian Gulf" (Apart). And the transportation sector is the largest source of greenhouse gas emissions according for 29% of all the emission (environmental protection agency). As a result, eco-driving has spawned, and it is an initiative which has seen worldwide adoption and investigation in the past decade (Alam and McNabola, 2014). Eco-driving is a driving pattern which emphasizes the combination of velocity, safety, fuel efficiency and air emission (Killian, 2012). In this paper, we propose the advisory speed limit (ASL), a method which was applied to smooth the stop-and-go traffic (Yang and Jin, 2014) to achieve eco-driving. A connected vehicle is a vehicle that can communicate bidirectionally with other systems outside of the vehicle (Elliott, 2014), it plays an important role in the study of eco-driving, which makes it possible to collect and share the environmental information and are the promising platform to realize eco-driving (Li et al., 2015). Therefore, we base our research on connected vehicles. The network fundamental diagram (NFD), a diagram that gives a relation between traffic flow-rate and density (Geroliminis and Daganzo, 2008), is chosen to be the approach of system mobility. The other indicator is the fuel consumption, and we choose Virginia Tech Microscopic Energy and Emission Model (VT-Micro model) (Ahn et al., 2002), a statistical model based on the real data, to calculate fuel consumption.

In order to build a relatively simple system, we first introduce Newell's car-following model (Newell, 1961, 2002). Under this condition, we assume that both of bounded acceleration and

bounded deceleration are infinite, and there is no reaction time for drivers. We then extend it to BA Newell's car-following model by considering bounded acceleration in starting-up process and bounded deceleration in the decision process of clearance behaviors (Jin and Laval, 2018). Drivers can be divided into two different styles under this condition: aggressive drivers and non-aggressive drivers. In order to guarantee safety, we assume all the drivers in our system are non-aggressive. Later we introduce intelligent driver model (IDM) (Treiber et al., 2000; Kesting et al., 2010) and study system mobility and fuel consumption based on it, we also compare the results of it with those of Newell's car-following model and BA Newell's car-following model.

In recent years, research on eco-driving algorithms has been ongoing. The major control objectives of eco-driving are acceleration/deceleration (Larsson and Ericsson, 2009), driving speed (Rakha and Kamalanathsharma, 2011) and route choice (Strömberg et al., 2015). The methods for eco-driving can be categorised into three groups, namely strategic decisions (vehicle selection and maintenance), tactical decisions (route planning and weight) and operational decisions (driving style) (Huang et al., 2018).

Speed is a widely utilized control objective in eco-driving, as early as 2005, Hegyi & Schutter & Hellendoorn began to design algorithms of dynamic speed limits on a freeway based on shock waves (Hegyi et al., 2005). Rskha & Kamalanathsharma developed a strategy yielding the most fuel-optimal speed profile for a vehicle approaching a signalized intersection using V2I communication capabilities (Rakha and Kamalanathsharma, 2011), and Katsaros & Kernchen & Dianati & Riech proposed a Green Light Optimized Speed Advisory (GLOSA) and evaluated its performance and efficiency (Katsaros et al., 2011). Later, Yang & Jin proposed a green driving strategy based on feedback control theory and infrastructure vehicle communication (Yang and Jin, 2014). He & Liu & Liu took queue phenomenon in to consideration and proposed a multi-stage optimal control formulation to obtain the optimal vehicle trajectories on signalized arterials (He et al., 2015). Luo & Li & Zhang & Qin & Li proposed a novel optimal speed advisory strategy for continuous intersections suitable for hybrid electric vehicles (Luo et al., 2017). Yao & Cui & Li & Wang & An also proposed a novel vehicle trajectory smoothing method (i.e. IVSL-LC) on the approaching link of a fixed-time signalized intersection (Yao et al., 2018).

There are also many studies about the evaluation of eco-driving algorithms. In 2007, Kwon & Brannan & Shouman & Isackson & Arseneau observed the influence that the advisory speed

limit can bring to speed and total throughput volume during peak hours on the basement of the data in Twin Cities, Minnesota (Kwon et al., 2007). Later Nissan & Koutsopoulosb derived a statistical method for the evaluation of the impacts of variable speed limits on traffic operations of a facility (Nissan and Koutsopoulosb, 2011), and Elvik studied the connection between speed limits and safety issues (Elvik, 2012). Eckhoff & Halmos & German began to investigate the limitations of Green Light Optimized Speed Advisory (GLOSA) under over-congested conditions from the perspective of travel time (Eckhoff et al., 2013). One year later, Jalooli & Shaghaghi & Jabbarpour & Noor & Yeo & Jung demonstrated the efficiency of Intelligent Advisory Speed Limit Dedication(IASLD) in improving traffic flow and reducing average travel time (Jalooli et al., 2014).

The inspiration for this study comes from the static ASL algorithm proposed by Ubiergo & Jin (Ubiergo and Jin, 2016); the core goal of the ASL is to better utilize the phase time and smooth the stop-and-go traffic. However, because of safety issues, the static ASL algorithm may not be able to work well; thus we propose the dynamic ASL algorithm based on Ubiergo & Jin's work. In order to evaluate our algorithm, we conduct the simulation and derive corresponding network fundamental diagrams, we demonstrate that our algorithm can increase the system mobility, especially under saturated condition. We also show that our algorithm can reduce the fuel consumption with VT-micro model approach.

In addition, according to the principles of algorithm designing, our algorithm should work even when there is only one connected vehicle adopting our algorithm, but with a higher market penetration rate (MPR) the algorithm should perform better. Thus we take MPRs of connected vehicles into consideration; we detect the influence to system mobility as well as fuel consumption brought by different MPRs. The other element we focus on is the length of the ASL implementation area, the algorithm is supposed to perform better with a larger implementation area, however, the computation cost will also increase. Therefore, we find the minimum implementation area that can guarantee the efficiency of our algorithm.

The main contribution of our study can be summarized into three aspects. Firstly, there have been many studies on the ASL from the perspective of environmental protection, however, people haven't used the NFD to evaluate the ASL and we fill this blank, thus we can detect the efficiency of the ASL under different congestion levels. Secondly, we proposed a new dynamic ASL al-

gorithm and proved the efficiency of it. Finally, we study how the market penetration rate and the ASL implementation area can affect the algorithm efficiency and propose suggestions for the application of the algorithm.

The rest of this paper is organized into 6 sections. In section 2, we will analyze the current static ASL algorithm as well as propose our own dynamic ASL algorithm. In section 3, we will introduce the driving behavior models. In section 4, we will theoretically introduce the performance measurements of our algorithm. In section 5, we will set up the simulation, conduct the simulation and show corresponding results. In section 6, we will take the market penetration rate (MPR) as well as the ASL implementation area in to consideration. And finally, we will summarize the conclusions and discuss some potential extension of our research.

Chapter 2

Static and the dynamic advisory speed limit (ASL) algorithms

As a pioneer in the study of the advisory speed limit (ASL), Ubiergo & Jin proposed a static ASL algorithm (Ubiergo and Jin, 2016). We carefully studied and analyzed it and found some problems. This offer us the inspiration to develop the dynamic ASL algorithm.

2.1 Static ASL algorithm analysis

To reduce fuel consumption and gas emission, Ubiergo & Jin proposed a static ASL algorithm within the framework of a feedback control system (Ubiergo and Jin, 2016). The main goal of their algorithm is to reduce or even eliminate the lost time caused by start-up and clearance behaviors, and they want to achieve this goal through making vehicles enter the intersection during the phase time. Figure (1) provides a detailed process of their ASL algorithm.

Before going to the algorithm, we need to introduce the definition of saturation headway h and the ASL implementation area, which are utilized throughout the whole algorithm. Saturation headway h is the inverse of saturation flow-rate C, and saturation flow-rate is defined as the maximum flow rate for a traffic lane measured at the stop line during the green interval of a signalized intersection approach (Ranasinge et al., 2017). The ASL implementation area is an area on the entire road where vehicles will follow ASL instead of the original speed limit (v_f).

In their algorithm, with data collected by loop detectors, as well as information provided by

traffic signals, they are able to anticipate the expected arrival time of each connected vehicle at the intersection, $\Phi(n, \theta)$, where $\theta = \frac{t}{T}$ is the time in the unit of the cycle length T. With this value and the position and speed of a vehicle, say vehicle n, the 'ASL Equation' (formula (1)) provides an individual ASL for each connected vehicle to follow. For those connected vehicles, the vehicles' behaviors are modified by replacing the speed limit, v_f, by the ASL $v_{ASL}(n, \theta)$.

$$v_{ASL}(n, \theta) = \frac{L - X(n, \theta)}{(\Phi(n, \theta) - \theta)T} \tag{2.1}$$

$v_{ASL}(n, \theta)$ and $\Phi(n, \theta)$ are calculated for each vehicle every time when it enters the ASL implementation area. Figure 2(a) provides a sample for this control algorithm, if the first vehicle travels at the original speed limit (the blue discontinuous trajectory), it will enter the intersection during the red interval, in order to avoid coming across the red light, it should wait for the next green interval. Therefore, for the first vehicle, $\Phi(1, \theta)$ is the starting point of the next green interval, and $v_{ASL}(1, \theta)$ is calculated based on it; its velocity cannot exceed $v_{ASL}(1, \theta)$, otherwise it will enter the intersection at red interval and stop. The vehicle behind it is assigned a desired arrival time which is one saturation headway h after it (the green continuous line). Finally, vehicle 3 can enter the intersection travelling at original speed limit while also respecting the intersection capacity and the traffic light. For more detailed introduction, we refer to "(Ubiergo and Jin, 2016)" .

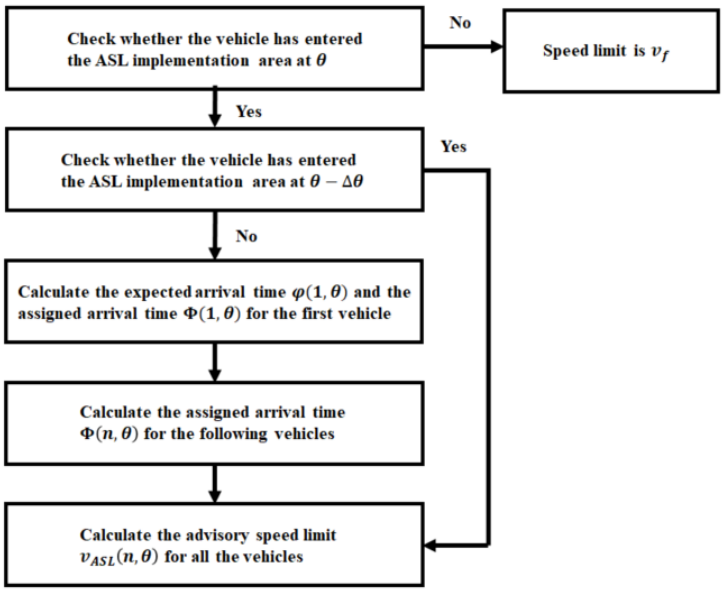

Figure 2.1: Flow Chart of Static ASL Algorithm

Nevertheless, if this algorithm is applied, vehicles cannot move as they expect when entering the intersection because of the security restrictions in car-following behaviors. In the reality, under saturated condition, when the front vehicle travels at a lower velocity, the vehicles will decelerate before they enter the intersection even its ASL is higher (as figure 2(b) shows), thus the actual headway is larger than saturation headway. Meanwhile, once one vehicle enters the intersection later than the assigned time, vehicles behind it will also be influenced. To summarize, these connected vehicles will follow lower speed constraints and still cannot enter the intersection at the assigned time, and such impacts are cumulative. As a result, the speed limit decreases, however, the stopping behaviors cannot be eliminated because the vehicles will not move following the ASL. Therefore, the average speed of each vehicle during the whole simulation also decreases and the same as the system average speed; the corresponding flow-rate will also decrease. To conclude, such cumulative influence will significantly impact the system mobility.

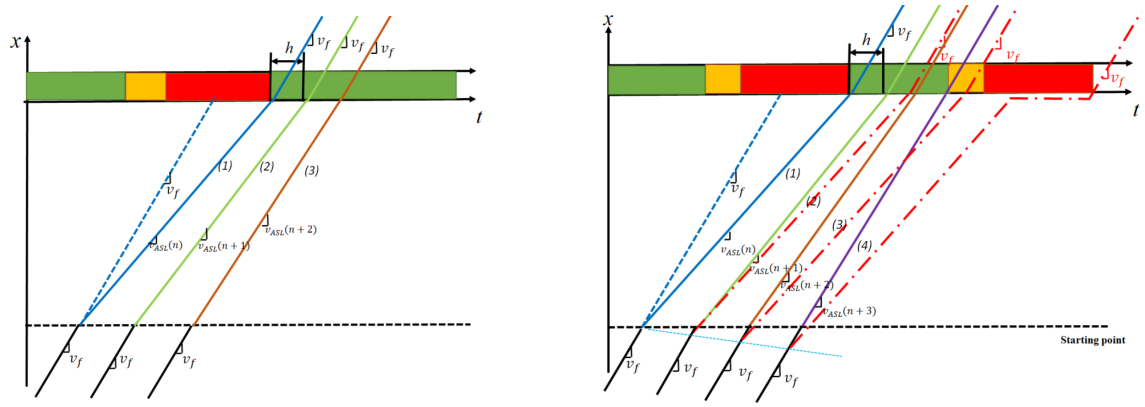

(a) (b)

Figure 2.2: (a) Expected Trajectories of the Static ASL, (b) Actual Trajectories of the Static ASL

Considering limitations of the static ASL algorithm, we develop the dynamic ASL algorithm by updating advisory speed limits dynamically.

2.2 Dynamic ASL algorithm

2.2.1 Algorithm introduction

Because the core goal of applying advisory speed limits to vehicles is to eliminate or at least to reduce the lost time caused by start-up and clearance behaviors. We intend to achieve this goal

through reducing the lost time in phase time, thus we control the time point at which a vehicle should enter the intersection. This process is done at each time-step once the vehicle enters the ASL implementation area, and this is the reason why we call this algorithm "dynamic".

Once a vehicle enters the intersection during red intervals, it must stop for some time, thus in order to avoid such phenomenon vehicles can only enter the intersection during the phase time in our algorithm. In our anticipation, vehicles enter the intersection during the phase time at one saturation headway (h) intervals, and the saturation headway (h) can be calculated in advance. Therefore, we can calculate a desired time for each vehicle to enter the intersection and update it at each time-step, and based on the desired arrival time, the dynamic ASL can be calculated, this will be clarified detailedly in the following part.

To summarize, the algorithm has to follow the principles and the assumptions below:

1) The algorithm is designed based on the ideal condition. For vehicles in the ASL implementation area, the first vehicle behind the stopping line is expected to enter the intersection at free-flow speed, and the vehicles behind it are designed to enter the intersection at saturation headway intervals.

2) The trajectories should be smoother after applying the algorithm, with less variation of vehicles' velocity, the fuel consumption can be reduced, which corresponds to the conception of "eco-driving".

3) Our algorithm should work even if there is only one connected vehicle adopting our algorithm. But with a higher market penetration rate of connected vehicles, our algorithm should have a better effect.

4) We assume that there is no random error in the system. That is, the GPS is totally accurate and there is no communication delay. Meanwhile, we assume that positions of all the vehicles (both connected vehicles and non-connected vehicles) are available.

5) The schematic diagram of the system is shown as Figure (3).

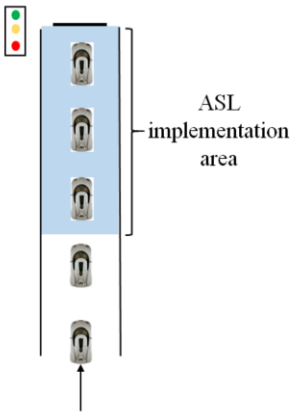

Figure 2.3: The Schematic Diagram of the System

2.2.2 Algorithm design

Based on the core idea, we developed a Dynamic ASL algorithm (DASL) at discrete time steps, a time step is equal to a time gap ($\Delta t = \tau$). On a ring road with length of L, the x-axis increases in the traffic direction, and we place a typical three-color signal at L. We assume the cycle length of the signal is T, and the green ratio is π. The original speed limit is free-flow speed v_f, ρ is jam spacing, $\theta = \frac{t}{T}$ is the time in the unit of a cycle length T, $\xi = \frac{h}{T}$ is the saturation headway h in the unit of a cycle length T, and $X(n, \theta)$ is the position of vehicle n at time θ. Focused on time θ, at each discrete time-step, the whole process can be summarized into four steps and it should be updated from time to time.

1. To begin with, we must specify the vehicles which are in the ASL implementation area. The dynamic ASL algorithm should be applied to those connected vehicles. X_s is the starting point of the ASL implementation area, for a vehicle n, if $X(n, \theta) \geq X_s$, it has already entered the ASL implementation area. If a vehicle is in the implementation area, we continue to calculate the dynamic ASL. Otherwise it is constrained by the original speed limit (v_f).

2. We define the "first vehicle" (say vehicle 1), the "first vehicle" is the vehicle which is the closest to the stopping line; and its expected arrival time ($\varphi(1, \theta)$) when it travels at original speed limit is calculated:

$$\varphi(1, \theta) = \theta + \frac{L - X(1, \theta)}{v_f T} \tag{2.2}$$

The corresponding desired arrival time for the "first vehicle" can be calculated:

$$\Phi(1,\theta) = \begin{cases} \varphi(1,\theta), & \varphi(1,\theta)\ mod\ 1 < \pi \\ \lfloor \varphi(1,\theta) \rfloor + 1, & otherwise \end{cases} \tag{2.3}$$

If the vehicle is expected to arrive at the intersection at a green interval, the desired arrival time is equal to the expected arrival time; otherwise the desired arrival time is the beginning point of the next green interval.

3. In the third step, we work out desired arrival time for the following vehicles. According to our design, as mentioned in section 2.2.1, vehicles behind the "first vehicle" should enter the intersection at saturation headway (h) intervals. For example, the saturation headway in Newell's car-following models can be calculated through: $h = \tau + \frac{\rho}{v_f}$. However, if a vehicle is designed to enter the intersection at the end of one phase time ($m + \pi$, m is a positive integer), the vehicle behind it can enter the intersection at the beginning of the next green interval ($(m + 1)$), that is, the time interval between such two vehicles will be less than $(1 - \pi) + \xi$. Therefore, the desired arrival time for the following vehicles (vehicle 2 to vehicle n) in the ASL implementation area can be calculated based on the front vehicles:

$$\Phi(n,\theta) = \begin{cases} \Phi(n-1,\theta) + \xi, & [(\Phi(n-1,\theta) + \xi)\ mod\ 1] < \pi \\ \lfloor \Phi(n-1,\theta) + \xi \rfloor + 1, & otherwise \end{cases} \tag{2.4}$$

The time interval between the adjacent two vehicles to enter the intersection should be a saturation headway h, but if a red interval is equal to or less than a saturation headway h from the desired arrival time of its preceding vehicle, the following vehicle can enter the intersection at the starting point of next green interval.

4. In the fourth step, we calculate the ASL for each vehicle:

$$v_{ASL}(n,\theta) = min\{v_f, \frac{L - X(n,\theta)}{(\Phi(n,\theta) - \theta)T}\} \tag{2.5}$$

The advisory speed limit for a vehicle is calculated based on its current position as well as

the desired arrival time; however, it cannot exceed the original speed limit.

The whole process of our algorithm can be summarized as figure (4).

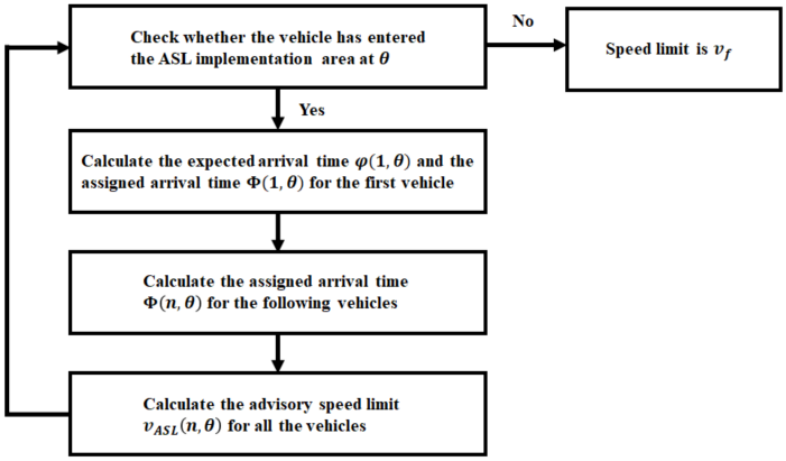

Figure 2.4: Flow Chart of Dynamic ASL Algorithm

2.2.3 Algorithm analysis and anticipation

In the dynamic ASL algorithm, the ASL is calculated and updated at each time-step based on current location and signal status. For vehicles in the implementation area, it is possible for them to decelerate at first and then accelerate again. Therefore, it can solve the problem caused by the static ASL algorithm, and will not result in the cumulative delay when vehicles enter the intersection.

According to the algorithm, once a vehicle enters the ASL implementation area, its speed limit is calculated based on the ideal condition, and adjusted and updated based on the actual situation at every moment. Therefore, in our anticipation, when roads are not over congested and all the vehicles are connected vehicles, stopping behaviors can be totally eliminated. That is, at the beginning of a green interval, the first vehicle to go through the intersection does not need to accelerate from zero, and thus the corresponding headway between two vehicles will be reduced. Meanwhile, for all the vehicles are to enter the intersection during this interval, the actual headway of them and the preceding vehicles will decrease. Meanwhile those vehicles will not be influenced by reaction time, this can further decrease the actual headway between two adjacent vehicles; therefore, from this perspective, the system mobility will be further improved in our

anticipation. However, with the existence of the bounded acceleration, the lost time cannot be reduced to zero.

Comparing to the original driving behaviors, after applying the dynamic ASL algorithm, the speed profiles for connected vehicles will be much smoother than those before; thus from this perspective, the fuel consumption will also be reduced.

Chapter 3

Driving behavior models

For simulating vehicle movements, we need to introduce car-following models. In this section, we introduce three models: Newell's car-following model, BA Newell's car-following model and intelligent driver model (IDM).

3.1 Newell's car-following model

In order to study the effect of the ASL on the road performance, it is necessary to study the road performance without ASL as a control group. We chose to begin with the simplest condition which is the easiest to get theoretical results. Newell's car-following model is derived from LWR model and it is equivalent to the LWR model regardless of the bounded acceleration (Lighthill and Whitham, 1955), at every time step in the simulation, the car-following model updates the vehicle's speed and the position as formula (6) and (7):

$$v(n, t + \Delta t) = min\{\frac{X(n - \Delta n, t) - X(n, t) - \rho\Delta n}{\tau\Delta n}, v_f\} \tag{3.1}$$

$$X(n, t + \Delta t) = min\{X(n, t) + \Delta t v_f, X(n, t) + \Delta t \times \frac{X(n - \Delta n, t) - X(n, t) - \rho\Delta n}{\tau\Delta n}\} \tag{3.2}$$

Where v_f is free-flow speed, $\tau = 1/(wk_j)$ is the time gap, k_j is the jam density and $\rho = 1/k_j$ is the jam spacing. In Newell's car-following model, all the vehicles are assumed to move on a

homogeneous road, the trajectory of the following vehicle is the same as that of the front vehicle; and all the vehicles will maintain minimum spaces and time gaps between themselves and the proceeding vehicles. Meanwhile, the velocity is also constrained by the speed limit v_f.

3.2 BA Newell's car-following model

In the reality, the speed of a vehicle is impossible to significantly change in a very short time, it is limited by the bounded acceleration. In order to make the simulation more realistic, bounded acceleration is added to the model as the start-up behavior. This model with start-up behaviors is defined as BA Newell's car-following model (Jin and Laval, 2018). The formulas can be written as:

$$v(n, t + \Delta t) = min\{\frac{X(n - \Delta n, t) - X(n, t) - \rho \Delta n}{\tau \Delta n}, v_f, v(n, t) + \Delta t a_0\} \tag{3.3}$$

$$X(n, t + \Delta t) = min\{X(n, t) + \Delta t v_f, X(n, t) + \Delta t \times \frac{X(n - \Delta n, t) - X(n, t) - \rho \Delta n}{\tau \Delta n}, X(n, t) + \Delta t v(n, t) + \Delta t^2 a_0\} \tag{3.4}$$

Where a_0 is the bounded acceleration. BA Newell's car-following model sets a constraint for acceleration, the acceleration cannot exceed a_0.

3.3 Intelligent driver model

In Newell's car-following model and BA Newell's car-following model, bounded deceleration is only considered during the decision process; in the implementation process, however, deceleration is not bounded. Because we choose VT-micro model (Ahn et al., 2002) to describe fuel consumption; it is a statistical model based on real data and its detailed introduction is referred to section 4.3. According to the concept and formulas of VT-micro model, there will be some problems if the deceleration is unbounded and fuel consumption can be exponentially increasing. For example, when the deceleration is $15m^2/s$, fuel consumption can be nearly $2.4 \times 10^{77} liter/sec$, which means that a vehicle will use up all the fuel suddenly. Therefore, considering the reality, we also introduce intelligent driver model (IDM).

IDM was first published by Treiber, Hennecke and Helbing; it can provide collision-free behaviors and self-organized characteristics (Treiber et al., 2000; Kesting et al., 2010). It assumes that the dominant influence on driving behavior comes from the vehicle ahead (Kesting, 2008). The discrete time IDM can be expressed as:

$$a(n,t) = max\{-b, a_0\big[1 - (\frac{v(n,t)}{v_f})^{\delta} - (\frac{s^*(n,t)}{s(n,t)})^2\big]\} \tag{3.5}$$

$$v(n,t+\Delta t) = max\Big\{0, min\{v_f, v(n,t) + a(n,t)\Delta t\}\Big\} \tag{3.6}$$

$$x(n,t+\Delta t) = max\Big\{x(n,t), min\{x(n,t) + v_f\Delta t, x(n,t) + v(n,t)\Delta t + \frac{a(n,t)\Delta t^2}{2}\}\Big\} \tag{3.7}$$

Where v_f is the desired velocity, δ is the acceleration exponent, a_0 is the desired maximum forward acceleration and b is the absolute value of the desired maximum braking deceleration. $s^*(n,t)$ and $s(n,t)$ are a desired distance gap and an actual distance gap of vehicle n at time t respectively. They can be calculated through:

$$s(n,t) = x(n-\Delta n, t) - x(n,t) - l_n \tag{3.8}$$

$$s^*(n,t) = s_0 + v(n,t) \times \tau + \frac{v(n,t)\big[v(n,t) - v(n-\Delta n,t)\big]}{2\sqrt{a_0 b}} \tag{3.9}$$

Where l_n is the length of vehicle n, s_0 is the minimum bumper-to-bumper distance, τ is the safe time gap. The acceleration exponent shows how the acceleration decreases when approaching the desired velocity, only when $\delta \to \infty$ the speed approached the desired velocity with a constant acceleration. We set $\delta = 4$ throughout the simulation because this corresponds to the most realistic acceleration behavior.

3.4 Start-up behaviors

As mentioned in section 3.2, start-up behaviors are influenced by bounded acceleration; meanwhile, reaction time is also an important element. "Reaction time" is defined as the interval of time between presentation of stimulus and appearance of appropriate voluntary response in a subject. The receipt of information (visual or auditory), its processing, decision making, and giving the response or execution of the motor act are the processes which follow one another and make what we call the "reaction time" (Balakrishnan et al., 2014). Because of the reaction time, drivers cannot change their movement status immediately when the signal changes from red to green; in other words, they will maintain their current status for some time until they react to the external changes.

According to (Roess et al., 2011), the start-up lost time for queued vehicles decreased significantly by location; therefore, we assume that only the leading vehicle is influenced by the start-up reaction time, and only when a vehicle is stopped, it will be influenced by the reaction time when the signal changes from red to green.

3.5 Clearance behaviors

Before introducing clearance behaviors, the dilemma zone should be eliminated first. The dilemma zone is widely known as an area on the high-speed intersection approach, where vehicles neither safely stop before the stop line nor proceed through the intersection during amber interval (Zhang et al., 2014). It can be eliminated when the yellow plus all-red interval is long enough. The principle is shown as below:

$$Y \geq t_{RE} + \frac{v_f}{2b} + \frac{L_{int}}{v_f} \tag{3.10}$$

Where L_{int} is the length of the intersection, Y is the yellow plus all-red interval, t_{RE} is the reaction time and b is the bounded deceleration.

In Newell's car-following model, no bounded acceleration is introduced, a vehicle can reach the speed limit or stop immediately, thus there is no dilemma zone under this condition and those

vehicles do not need to make a decision before the signal changes to red. To summarize, for Newell's car-following model, at the time point the signal changes to red from the phase time, all the vehicles which have passed the intersection can remain the moving states and the others should stop. For those vehicles which have not gone through the intersection, the vehicle which is the closest to the stop line will be the one to follow the signal states and the vehicles behind it will follow their front vehicles. However, for the other two models, clearance behaviors should be discussed. One thing should be noted is that the front bumper of the first vehicle can reach the stop line, however, the vehicles behind the first vehicle must be at least jam spacing from the front vehicles when they stop.

3.5.1 Stopping condition

Bounded deceleration is considered in the decision process when the signal changes to yellow from green. According to the bounded deceleration, the distance between the vehicle and the intersection and the distance needed for braking can be calculated through formula (16) and (17) (Morales Fresquet and Jin, 2018) .

$$D_{veh-int} = X_{int} - X(n,t) \tag{3.11}$$

$$D_{Stop} = t_{RE} \times v(n,t) + \frac{v(n,t)^2}{2b} \tag{3.12}$$

If $D_{veh-int} > D_{Stop}$, the vehicle can stop.

Where X_{int} represents the position of the intersection, $X(n,t)$ represents the position of vehicle n at time t and $v(n,t)$ is the speed of vehicle n at time t. However, in Newell's car-following model and BA Newell's car-following model, this maximum deceleration rate is not considered in the implementation process, it will only affect the "can go decision". In other words, because there is no limit for the deceleration in two Newell's car-following models, a higher deceleration rate is possible and can even be infinite.

3.5.2 Crossing condition

The crossing condition means that a vehicle can go through the intersection before the signal changes to red if it remains at current speed. The distance between the vehicle and the intersection and the distance a vehicle can cover before the red light can be calculated through formula (18) and (19) (Morales Fresquet and Jin, 2018).

$$D_{veh-int} = X_{int} + L_{int} - X(n,t) \tag{3.13}$$

$$D_{Run} = v(n,t) \times Y \tag{3.14}$$

If $D_{veh-int} < D_{Run}$, the vehicle can go through.

3.5.3 Aggressive and non-aggressive behaviors

Since the stopping condition and the crossing condition exist, there may be some vehicles that can both stop or go through. Thus there are two types of clearance behaviors: aggressive and non-aggressive.

Aggressive drivers will stop only if they cannot go through the intersection; otherwise, if they satisfy both conditions, they will choose to go through the intersection. According to this condition, when the signal changes to yellow from green, test whether vehicles can go through the intersection at current speed; the first vehicle that cannot go through will be the first vehicle that needs to stop and therefore it should follow the stop line.

Non-aggressive drivers will go through the intersection only if they cannot satisfy the stop condition, otherwise they will stop. According to this condition, those drivers' test whether their vehicles satisfy the stop condition when the signal changes to yellow from green; the first vehicle that satisfies the stop condition will be the first vehicle that need to stop and it should follow the stop line.

In order to make our simulation controllable and to guarantee safety, we assume that all the drivers in our system are non-aggressive.

3.5.4 Decision tree

We assume that the dilemma zone is already eliminated, every time the signal changes from a green interval to a yellow interval, the decision process of drivers can be represented by the figure (5).

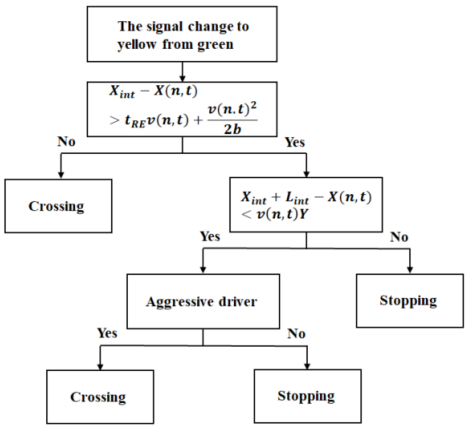

Figure 3.1: Decision Process When the Signal Changes to Yellow from Green

Where t_{RE} is the reaction time, L_{int} is the length of the intersection, Y is the yellow plus all-red interval, b is the bounded deceleration, X_{int} is the position of the intersection, $X(n,t)$ is the position of vehicle n at time t and $v(n,t)$ is the speed of vehicle n at time t.

Chapter 4

Network fundamental diagram and emission model

In order to test the effectiveness of our algorithm, we need some evaluation indicators. We intend to prove that our algorithm can not only reduce the environmental effect, but also improve the system mobility, thus we select the network fundamental diagram (NFD) and fuel consumption as evaluation indicators.

4.1 The detection of velocity periodicity

In order to determine the simulation period when deriving NFDs, we need to study the periodicity of velocity. According to Jin & Yu (2015) (Jin and Yu, 2015b), it can be found that the periodic phenomena occur frequently for individuals and signalized systems after reaching the stationary state. And they have found that the minimum period might be a multiple of the cycle length T instead of just T (Jin and Yu, 2015a).

According to our study, individual vehicles have their own periods ($T_N(n)$, the unit for $T_N(n)$ is a second) after the system reaches the stationary state, periods of different individual vehicles are the same under one specific density, but such periods may not be the same as the period (T'_N) of system average speed. This can be clarified by an example, we take vehicle number is 40 as an example, and plot the speed profiles of vehicle 1 and vehicle 10 as well as the system average speed. It can be found that under such condition, the period for individuals is $10T$ and the

period for the system average speed is T, as figure 6(a) shows. From the figure we can find that individuals have different periods from the system average speed, and the periods of individuals are the same, in other words, the speed profile of vehicle 10 can be gained by shifting the speed profile of vehicle 1. This is proved in figure 6(b), from the simulation we know that the time interval between vehicle 1 and vehicle 10 is 321 time-steps, and we shift back the speed profile of vehicle 1 by 321 time-steps; it can be seen from figure 6(b) that the speed profiles of two vehicles coincide with each other. All the vehicles cover the same distance in one period of individual vehicles $T_N(n)$, and they will experience the same pattern of the moving process. Therefore, we can use the fuel consumption of the first vehicle in one individual period to represent the system fuel consumption level.

In our study, when deriving network fundamental diagrams (NFD), the speed is only utilized for the calculation of flow-rate, thus we do not need to detailedly describe the instantaneous speed at each time-step. Because Jin & Yu have demonstrated that the minimum period is a multiple of the cycle length, in order to simplify the calculation, we calculate the average speed in each cycle length and find the period of such average speed. The average speed of vehicle n in one cycle length can be calculated through:

$$\bar{v}(n, mT) = \frac{X(n, (m+1)T) - X(n, mT)}{T} \tag{4.1}$$

Where m is a non-negative integer, T represents the cycle length, $\bar{v}(n, mT)$ represents the average speed of vehicle n in the m_{th} cycle length and $X(n, (m+1)T) - X(n, mT)$ represents the distance this vehicle can cover in the m_{th} cycle length. According to our simulation, the period of one individual can be really large, especially when the system is over congested, and we find that the period of the system average speed is much smaller and more stable. Thus considering the accuracy and cost-efficiency, we decide to derive NFD through the system average speed. We can calculate the system average speed ($\bar{v}'(mT)$) in the m_{th} cycle length through:

$$\bar{v}'(mT) = \frac{\sum_N \bar{v}(n, mT)}{N} \tag{4.2}$$

Where N is the total vehicle number.

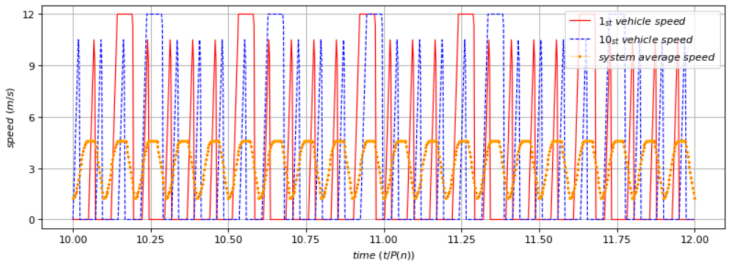

(a)

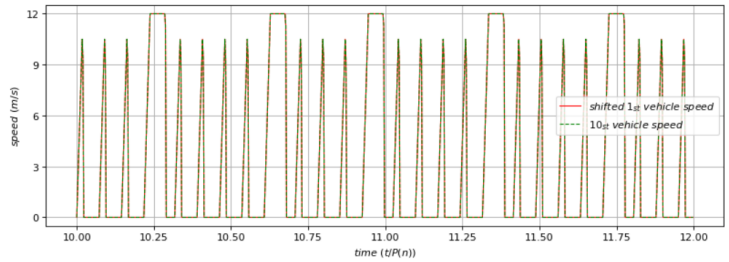

(b)

Figure 4.1: (a) Speed Profiles of Vehicle 1, Vehicle 10 and the System Average Speed (b) Speed Profiles of Shifted Vehicle 1 and Vehicle 10

Because the periodicity only appears after the speed convergences, and based on the simulation we found that the system reaches the stationary state approximately 50 minutes after the start of simulation. Thus the first 60 minutes during the simulation are abandoned. The period of system average speed and the period of individual speed can be calculated through formula (22) and (23) respectively. Assume there are M cycles during the simulation in total, we use m to represent the number which can be shifted along the cycle numbers, m is shifted forward from the last cycle length, we shift m along up to 30 cycle numbers for calculating the period of system average speeds and 100 cycle numbers for calculating the period of individual average speeds. If there exists some integers i that can satisfy formula (22) or (23) for any m, we consider that those integers are the periods of the stationary state for corresponding cycle length T and density k, and the final i is the smallest number among those integers.

$$\max_{m\in((M-30),M]} \frac{|\bar{v}'(mT) - \bar{v}'((m-i)T)|}{\pi C} < 10^{-5} \tag{4.3}$$

$$\max_{m\in((M-100),M]} \frac{|\bar{v}(1,mT) - \bar{v}(1,(m-i)T)|}{\pi C} < 10^{-5} \tag{4.4}$$

When deriving network fundamental diagrams we calculate the average flow-rate at corre-

sponding densities with the system average speed. And we use individual periods when calculating fuel consumption.

4.2 Network fundamental diagram

The network fundamental diagram of a system is a diagram that gives a relation between the traffic flow and traffic density (Geroliminis and Daganzo, 2008). It can be utilized to predict the capability of the system when applying inflow regulation or speed limits, thus it is chosen to be one of the approaches for our algorithm.

In this simulation, the simulation duration σ of all the vehicles are the same, assume there are N vehicles in the system, flow-rate can be calculated through:

$$\bar{q}(k) = k\bar{v}_a(k) \tag{4.5}$$

Where $\bar{v}_a(k)$ is the system average speed in one period at density k. The representation of NFD is displayed as figure (7), where π is the green ratio and C is the saturation flow-rate when there is no signal.

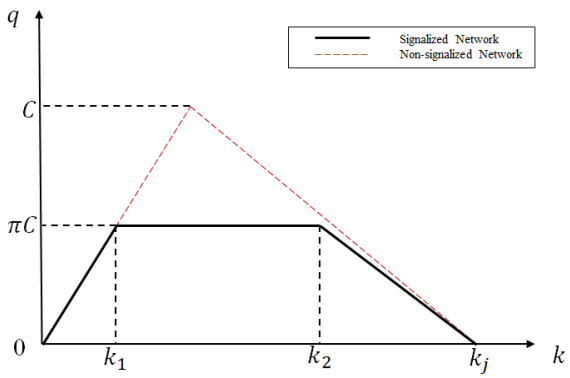

Figure 4.2: The Representation of The Network Fundamental Diagram

Jin & Yu have already derived the theoretical results for the fundamental diagram of original Newell's car-following model on a signalized road (Jin and Yu, 2015b). The green ratio π is set as 0.5 in this simulation, instead of a triangular fundamental diagram, the fundamental diagram will be approximated by a piecewise linear function. Compared with the single point of maximum flow-rate when the green ratio is 1, when the green ratio is 0.5, the maximum flow-rate will be a

horizontal line segment, and the ratio of the maximum flow-rate under two conditions is equal to the green ratio. The critical densities can be calculated through:

$$\frac{L}{v_f} = \theta_1 T,\ \theta_1 = j_1 + \alpha_1,\ j_1 = |\frac{L}{v_f T}| = 0, 1, ...,\ 0 < \alpha_1 \leq 1 \tag{4.6}$$

$$\frac{L}{w} = \theta_2 T,\ \theta_2 = j_2 + \alpha_2,\ j_2 = |\frac{L}{wT}| = 0, 1, ...,\ 0 < \alpha_2 \leq 1 \tag{4.7}$$

$$k_1 = \frac{j_1 + min\{\frac{\alpha_1}{\pi}, 1\}}{j_1 + \alpha_1} \times \pi k_c = (j_1 + min\{\frac{\alpha_1}{\pi}, 1\})\frac{\pi CT}{L} \tag{4.8}$$

$$k_2 = k_j - \frac{j_2 + min\{\frac{\alpha_2}{\pi}, 1\}}{j_2 + \alpha_2} \times \pi \frac{C}{w} = k_j - (j_2 + min\{\frac{\alpha_2}{\pi}, 1\})\frac{\pi CT}{L} \tag{4.9}$$

Where L is the road length, v_f is the free-flow speed (also the speed limit), $w = \frac{1}{\tau k_j}$ is the speed of the refraction wave and C is saturation flow-rate of the system when there is no signal.

4.3 VT-micro model for estimating fuel consumption

In consideration of the simplicity, accuracy, and ease of implementation, we use Virginia Tech Microscopic Energy and Emission Model (VT-Micro) to describe environmental influence. It is a regression model which considers a combination of linear, quadratic, and cubic speed and acceleration terms. Those terms were tested using the chassis dynamometer data collected at Oak Ridge National Laboratory (ORNL); this time we utilize fuel consumption to detect environmental influence of our algorithm. This model provides the least number of terms with a relatively good fit to the original data (R^2 in excess of 0.92 for all measures of effectiveness (MOE)) (Ahn et al., 2002; Rakha et al., 2003; Ahn and Rakha, 2008). The model has the following form:

$$MOE_e = \begin{cases} e^{\sum_{i=0}^{3}\sum_{j=0}^{3} L_{i,j}^{e} \times v^i \times a^j}, & for\ a \geq 0 \\ e^{\sum_{i=0}^{3}\sum_{j=0}^{3} M_{i,j}^{e} \times v^i \times a^j}, & for\ a < 0 \end{cases} \tag{4.10}$$

Where MOE_e is the instantaneous fuel consumption (l/s), $L^e_{i,j}$ and $M^e_{i,j}$ are the regression model coefficient for MOE 'e' at speed power 'i' and acceleration power 'j', v is the instantaneous vehicle speed (km/h), and a is the instantaneous vehicle acceleration $(km/h/s)$ (Ahn et al., 2002). In order to create a simple enough condition, the vehicles utilized in our system are assumed to be composite, and the coefficients we utilize are the averages of 9 vehicle categories, as table (1) and table (2) show:

Table 4.1: Positive Acceleration Coefficient

Coefficient	$Constant$	$Acceleration$	$Acceleration^2$	$Acceleration^3$
$Constant$	7.734520000	0.229460000	-0.005610000	0.000097730
$Speed$	0.027990000	0.006800000	-0.000772210	0.000008380
$Speed^2$	-0.000222800	-0.000044020	7.90000×10^{-7}	8.17000×10^{-7}
$Speed^3$	1.09000×10^{-6}	4.80000×10^{-8}	3.27000×10^{-8}	-7.79000×10^{-9}

Table 4.2: Negative Acceleration Coefficient

Coefficient	$Constant$	$Acceleration$	$Acceleration^2$	$Acceleration^3$
$Constant$	-7.734520000	-0.017990000	-0.004270000	0.000188290
$Speed$	0.028040000	0.007720000	0.000837440	-0.000033870
$Speed^2$	-0.000219880	-0.000052190	-7.44000×10^{-7}	2.77000×10^{-7}
$Speed^3$	1.08000×10^{-6}	2.47000×10^{-8}	4.87000×10^{-8}	3.79000×10^{-9}

For a specific trip, the origin and the destination are determined, that is, the distance a vehicle should cover is determined. Therefore, we can use fuel consumption of one vehicle (the first vehicle) to move one meter to represent the fuel consumption level under such condition. Sometimes periods of individuals can be very large, thus we choose 100 cycle lengths as the upper bound of the periods in our simulation. Which means that in our simulation, if periods of individuals are less than 100 cycle lengths, we use fuel consumption of the first vehicle in one period as the representation of fuel consumption level; else if periods are larger than 100 cycle lengths, we calculate the average fuel consumption of all the vehicles during these 100 cycle lengths.

The fuel consumption level can be calculated through:

$$V(N) = \begin{cases} \sum_{\eta=\frac{\tau-T_N(1)}{\Delta t}}^{\frac{\tau}{\Delta t}} MOE_e(1,\eta)\Delta t, & for\ T_N(1) < 100T \\ \sum_{n=1}^{N} \sum_{\eta=\frac{\tau-100T}{\Delta t}}^{\frac{\tau}{\Delta t}} MOE_e(n,\eta)\Delta t, & for\ T_N(1) \geq 100T \end{cases} \tag{4.11}$$

Where N is the total number of vehicles in the system, Δt is the time-step size, η is time in the

unit of time-step size and T is the cycle length. Meanwhile, the corresponding distance ($D(N)$) vehicles have covered can be calculated through:

$$D(N) = \begin{cases} X(\sigma, 1) - X(\sigma - T_N(n), 1), & for\ T_N(1) < 100T \\ \sum_{n=1}^{N}(X(\sigma, n) - X(\sigma - 100T, n)), & for\ T_N(1) \geq 100T \end{cases} \tag{4.12}$$

Where σ is the simulation duration, $T_N(n)$ is the individual period of vehicle n. Then average fuel consumption to cover a unit distance (l/m) can be calculated through:

$$\bar{V}(N) = \frac{V(N)}{D(N)} \tag{4.13}$$

In order move a certain distance $D(N)$, the fuel we need is $V(N)$, thus the quotient of the two represents the fuel required for a car to travel per unit length.

Chapter 5

Simulation and results

5.1 The simulation setup

To begin with, we need to build the simulation system (as figure (3) shows), the following simulations are based on this system.

1) Road information: We want to simulate vehicles' behaviors in a signalized grid, to achieve this goal, we construct a signalized ring road with one lane and one typical three-color traffic light. The length of the ring road is $L = 720m$, the x-axis increases in the traffic direction and signals are placed at $x = 0$, L, $2L$, $3L$ etc., it is equivalent to an infinite one-way street without turning movements. Meanwhile, this system is also equivalent to a fixed segment, on which there is inexhaustible traffic flow.

   We construct the system in this way, so that there is inexhaustible traffic flow in the system; and we can wait for the system to reach the stationary state and study network fundamental diagrams.

2) Signal information: In our simulation, the cycle length is assigned to be $T = 60s$ and it is fixed, which contains a $24s$ green interval (G), a $6s$ yellow plus all red interval (Y) and a $30s$ red interval (R), thus the green ratio $\pi = \frac{G+Y}{T} = 0.5$. When the simulation begins, the signal starts with the green interval.

3) Vehicle information: The free-flow speed (v_f) is $12m/s$ and it is the original speed limit, time gap (τ) is $1.5s$, bounded acceleration (a) is $1m^2/s$, bounded deceleration (b) is $2m^2/s$.

In Newell's car-following model and BA Newell's car-following model, jam spacing (ρ) is $7m$; and in IDM the vehicle lengths (l_n) for all the vehicles are $5m$, and the minimum bumper-to-bumper distance (s_0) is $2m$. Thus the parameters for Newell's car-following models and IDM are consistent with each other and the results of them can be compared. To begin with, vehicles are evenly distributed on the ring road and labeled in a counterclockwise direction; and the vehicle which is the first one behind the stop line is labeled as the first vehicle. After the simulation begins, vehicles move clockwise.

4) Driver information: The reaction time for all the drivers (t_{RE}) is $0.5s$, and we assume that all the drivers are non-aggressive.

5) According to the velocity periodicity detection, the system reaches the stationary state after approximate 50 minutes, thus we set the simulation duration (σ) to be 3 hours and the first hour is not considered in the calculation of average speeds.

6) We define the 'ASL implementation area' as the area where the ASL is applied, to begin with, we assume the ASL implementation area is the first 300 meters behind the stop line.

In the simulation, we set Δn to be 1. Because we evaluate our algorithm with NFD approach, we need to traverse the density from 0 to near k_j. Based on the system we have created, the jam density k_j is $\frac{1}{\rho} = \frac{1}{7} veh/m$, thus the simulation starts from 2 vehicles until the number of vehicles is 102.

5.2 Results of the system mobility

According to formula (25) to (28) and the parameters in section 5.1, we can calculate the theoretical critical densities of original Newell's car-following model.

$$w = \frac{1}{\tau k_j} = \frac{1}{1.5 \times \frac{1}{7}} = \frac{14}{3} m/sec, \;\; v_f k_c = w(k_j - k_c), \;\; k_c = \frac{1}{50} veh/m$$

$$q_c = k_c \times v_f = \frac{1}{50} \times 12 = \frac{6}{25} veh/sec$$

$$j_1 = |\frac{720}{12 \times 60}| = 1, \; \alpha_1 = 0; \quad j_2 = |\frac{720}{\frac{14}{3} \times 60}| = 2, \; \alpha_2 = \frac{4}{7}$$

$$k_1 = (1+0) \times \frac{0.5 \times (12/25) \times 60}{720} = \frac{1}{50} veh/m = \frac{7}{50} k_j$$

$$k_2 = \frac{1}{7} - (2+1) \times \frac{0.5 \times (12/25) \times 60}{720} = \frac{29}{350} veh/m = \frac{29}{50} k_j$$

Network fundamental diagrams of three car-following models are pasted as figure (8), both densities and flow-rates are normalized. From the NFDs the influence to the system mobility brought by the ASL can be reflected. It can be found that for three car-following models, the static ASL algorithm has the same influence mode; it significantly influences the system mobility. Initially, this effect has not yet emerged, with increasement of densities, this effect begins to become apparent, especially it changes the flow-rate under saturated condition and the second critical density, and after the second critical density, the effect gradually disappears.

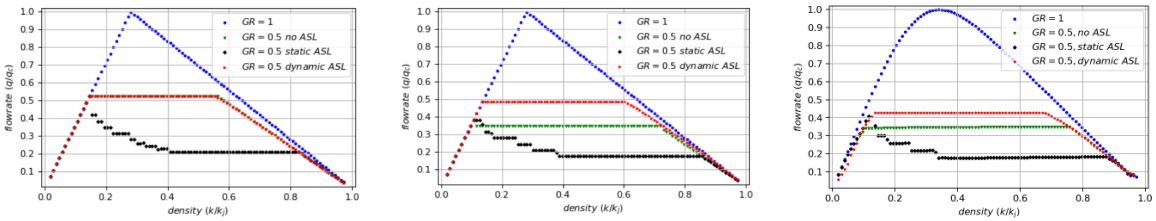

(a) (b) (c)

Figure 5.1: NFD of (a) Original Newell's Car-following Model, (b) BA Newell's Car-following Model, (c) IDM

Although the dynamic ASL makes little difference to the flow-rate for original Newell's car-following model. For BA Newell's car-following model and IDM, the flow-rate under saturated condition increases after the dynamic ASL is applied, this is consistent with our anticipation. However, after the second critical density, the benefit of the dynamic ASL to the system mobility gradually disappears. Meanwhile, with the existence of bounded acceleration, we can know that even if the dynamic ASL is applied, the capacity cannot reach $0.5C$; that is, the influence brought by start-up and clearance behaviors cannot be totally eliminated.

The influence of the dynamic ASL can also be reflected by vehicle trajectories. Through NFDs we can know that the dynamic ASL mainly plays a role under saturated condition, and according to the calculation above, the saturated condition corresponds to the condition when the vehicle number is 15 to 60. Therefore, we take the vehicle number is 40 as an example when studying trajectories, the results are shown as figure (9). We choose three conditions: without control, static ASL and dynamic ASL; and we plot the vehicle trajectories in the last five cycle lengths, the time

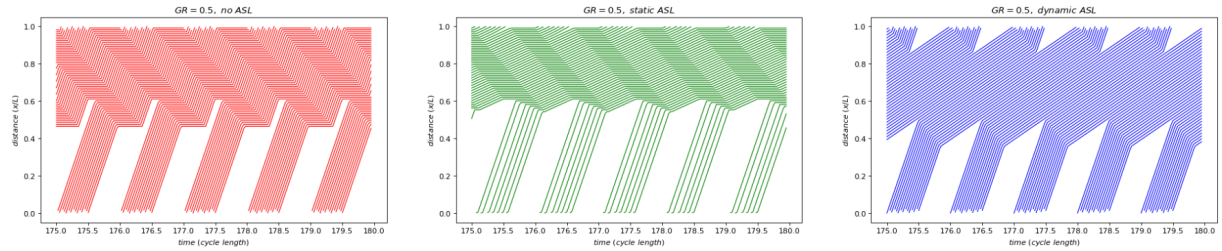

(a)

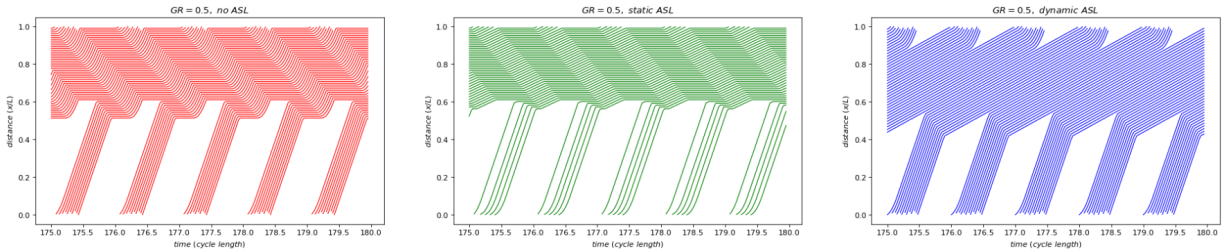

(b)

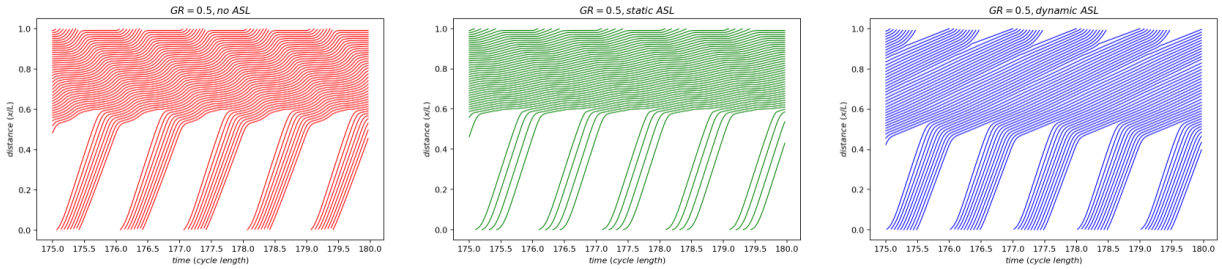

(c)

Figure 5.2: Vehicle Trajectories in the Last 5 Cycle Lengths of (a) Original Newell's Car-following Model, (b) BA Newell's Car-following Model and (c) IDM (Without Control, with Static ASL and with Dynamic ASL)

and the distance are normalized. From the trajectories it can be found that (i) the actual headway between two vehicles after applying the static ASL is much larger than saturation headway (h), (ii) stopping behaviors are totally eliminated after applying the dynamic ASL, (iii) the frequency of vehicles to go through the intersection increases after applying the dynamic ASL.

5.3 Results of fuel consumption

We choose fuel consumption as the measurement of environmental impact and utilize VT-micro model to calculate it. Both BA Newell's car-following model and intelligent driver model (IDM) are discussed in this section. We assume that all the vehicles in the system are connected vehicles, and calculate fuel consumption before and after applying the dynamic ASL.

The improvement rates of fuel consumption versus densities are plotted as figure (10). This

figure can be compared with figure (8), it can be found that the efficiency of the dynamic ASL has the same pattern from the perspective of system mobility and fuel consumption. The dynamic ASL is efficient under saturated condition, the improvement rate can reach up to approximate 25% and 100% based on IDM and BA Newell's car-following model respectively; and under the saturated conditions, the efficiency of the dynamic ASL can be maintained at a relatively stable improvement rate, neither over-saturated condition nor under-saturated condition can the algorithm contribute to the system.

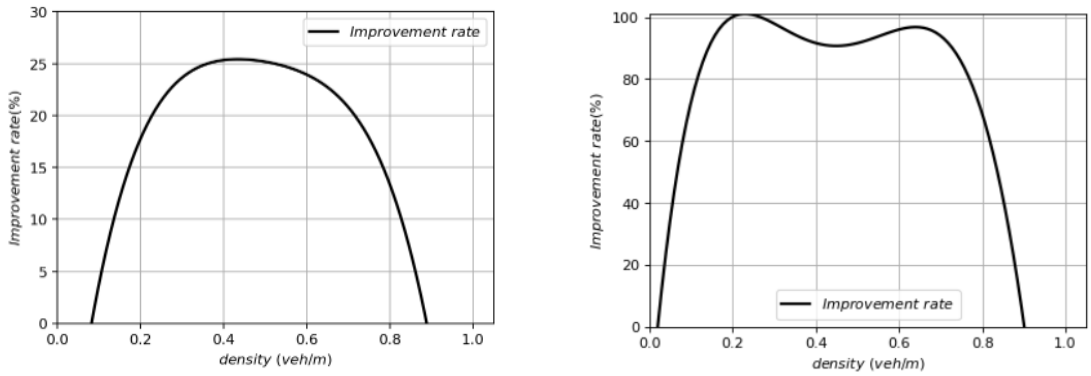

(a) (b)

Figure 5.3: Fuel Consumption Improvement Rate of (a) IDM, (b) BA Newell's Car-following Model

Chapter 6

Impacts of market penetration rates (MPR) and ASL implementation areas

According to the simulation results in section 5.2 and 5.3, for IDM, vehicles cannot move at speed limit (v_f) on freeway when flow-rate reaches the capacity, and the lost time on signalized road is too large. Thus comparing to IDM, BA Newell's car-following model is more suitable for the evaluation of system mobility. However, as mentioned in section 3.3, the fuel consumption can be very large when the deceleration is unbounded, and we can know from section 5.3 that the fuel consumption improvement rate of BA Newell's car-following model can reach 100%, which is unrealistic, thus BA Newell's car-following model is not very suitable for the evaluation of fuel consumption. Therefore, we choose BA Newell's car-following model for evaluating system mobility and IDM for fuel consumption.

6.1 Impact of MPRs

6.1.1 Monte Carlo Simulation

The Monte Carlo simulation is usually used when we need to predict the outcome of a process which contains the randomness and uncertainty, it can be used to minimize the influence brought by random elements. For a specific sampling distribution based on one population, we can get the density function of the values of this distribution, and then the estimate of this population is the frequency distribution of the values that were actually observed in many samples gain from this

population. However, it is impractical to sample actual values for many times in the reality, thus we can use some relevant methods to artificially generate the data (Mooney, 1997).

When market penetration rates are considered, some random elements are added into the system, and simulation results may differ from each other from time to time. Therefore, when studying the influence of MPRs, we simulate for fifty times and calculate the average value.

6.1.2 The impact brought by different MPRs

According to Yang & Jin 's work (Yang and Jin (2014)), we can know that substantial savings in vehicle emission and fuel consumption can be achieved when the market penetration rate (MPR) of connected vehicles is only 5%. Thus we take 5%, 10% and 70% MPRs of connected vehicles as examples, and study the corresponding system mobility and fuel consumption. Note that the position information and the estimated arrival time for all the vehicles, including those unconnected vehicles, should be available, otherwise unconnected vehicles will be "invisible" to the system; however, for those unconnected vehicles, the dynamic ASL algorithm will not be applied. The results are shown as figure (11).

The improvement of the system mobility is not obvious when the MPR is low. From figure 11(a) we can see that when the MPR is 5% or 10%, the corresponding NFDs show little difference. However, when the MPR increases to 70%, we can see obvious improvement in the system mobility; and when the MPR is 100%, the system mobility can be further improved.

Results of fuel consumption have the same pattern as those of system mobility. When the MPR is only 5%, we can see a certain improvement rate. As the MPR increases, the improvement rate also increases. The results about MPRs also conform to the principles of our algorithm.

The vehicle trajectories under different MPRs are plotted as figure (12), we consider both of BA Newell's car-following model and IDM. Note that as mentioned above, some stochastic elements exist in our simulation when considering the MPR, thus vehicle trajectories are only a sample. We still consider vehicle number is 40 and plot vehicle trajectories in the last five cycle lengths when the MPRs are 5%, 10%, 70% and 100%.

From the trajectories we can find that when the market penetration rate is low (like 5% or 10%), the stopping time of vehicles can already be reduced to a great extent, but stopping behaviors cannot be completely eliminated. In this case, when going through the intersection, vehicles

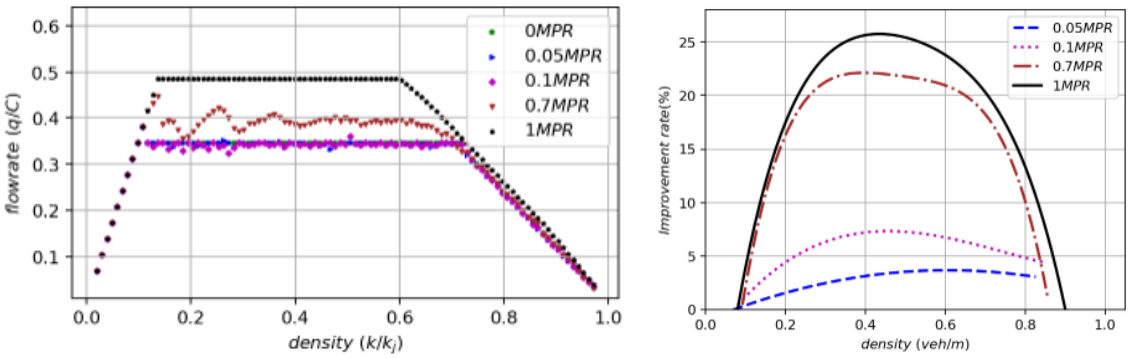

(a) (b)

Figure 6.1: (a) NFD of BA Newell's Car-following Model under Different MPRs, (b) Fuel Consumption of IDM under Different MPRs

still need to accelerate from zero, and drivers will be affected by the reaction time. Thus from the perspective of system mobility, when the MPR is very low, the impact is relatively limited. The dynamic ASL can make trajectories smoother, and the degree to which trajectories become smoother is positively related to the MPR, and therefore the improvement rate of fuel consumption is also positively related to the MPR.

6.2 Impact of ASL implementation areas

Generally speaking, it is good to apply the ASL as early as possible, because those connected vehicles can respond to the signal earlier. However, with a larger ASL implementation area, the computation cost will also increase. Therefore, on the premise of ensuring control results, we need to find the smallest ASL implementation area. Assume the MPR is 100%, because we have found that this algorithm mainly works under saturated condition and two critical densities correspond to vehicle numbers are 15 and 60 respectively, we take vehicle numbers are 30, 32, 35, 38 and 40 as examples, and set the ASL implementation area from 0 to 300 meters at intervals of ten meters.

The results are shown as figure (13), we can know from the results that when the ASL implementation area is less than 40 meters, the system mobility will be negatively influenced; and when the ASL implementation area is less than approximate 100 meters, the improvement rate of fuel consumption is no longer stable and cannot be fully guaranteed. Therefore, in order to guarantee control results as well as reducing computation cost, we recommend the ASL implementation area to be approximate 100 to 150 meters.

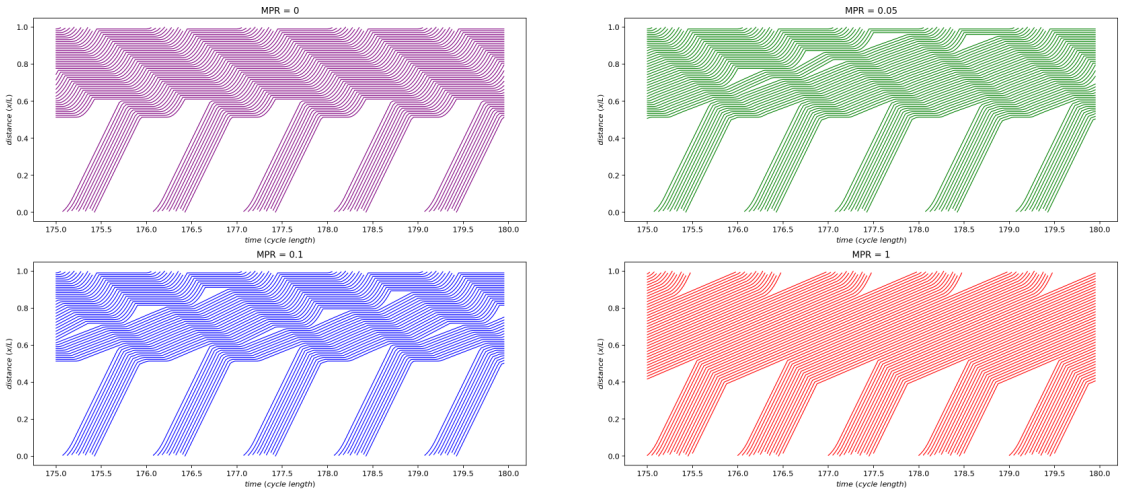

(a)

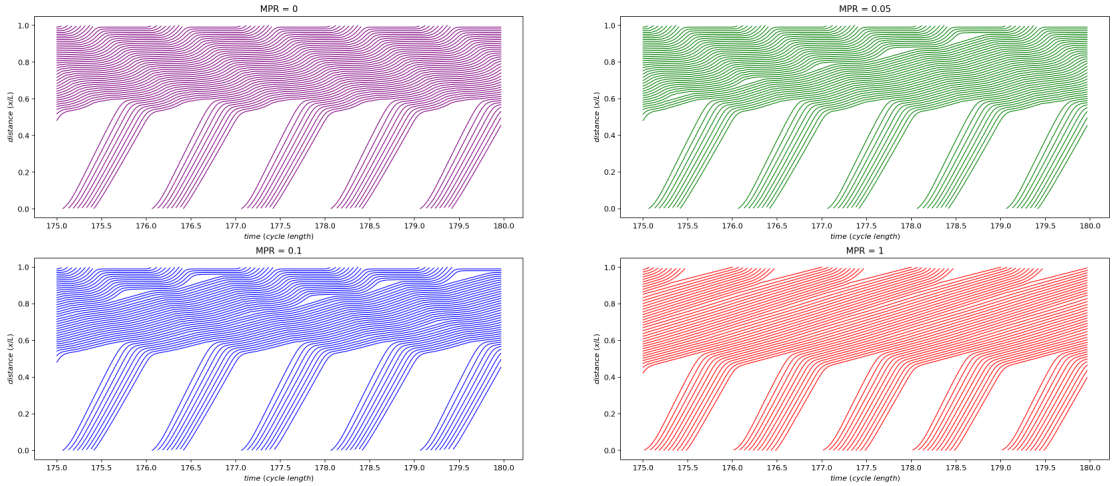

(b)

Figure 6.2: Vehicle Trajectories of (a) BA Newell's Car-following Model, (b) IDM in the Last 5 Cycle Lengths under Different MPRs

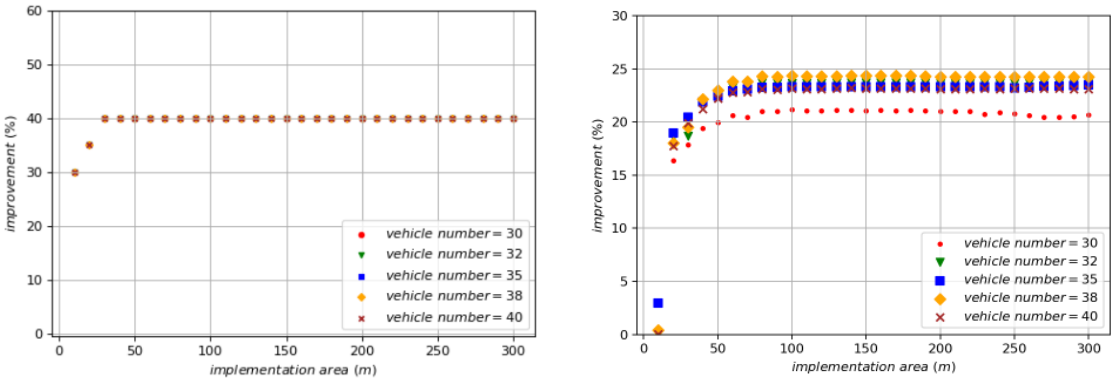

(a) (b)

Figure 6.3: The Improvement Rate of (a) System Mobility, (b) Fuel consumption along the ASL Implementation Areas

Chapter 7

Conclusion and future study

In this paper, we mainly propose a dynamic ASL algorithm and study the impact of it from the perspective of system mobility and fuel consumption; and we study influence to the efficiency of our algorithm brought by the market penetration rate and the ASL implementation area.

We first introduce some problems we may face in the implementation if we apply the static ASL algorithm, and show that this algorithm not only has little effect in eliminating start-up and clearance behaviors, but also negatively impacts the system mobility through simulation. Based on the analysis of the static ASL algorithm, we propose the dynamic ASL algorithm.

We analyze the efficiency of the dynamic ASL algorithm from the perspective of system mobility and fuel consumption, with network fundamental diagrams and VT-micro model approach. We show that this algorithm can improve system mobility and reduce fuel consumption under saturated condition. With proper car-following models, the improvement rate of system mobility can reach up to approximate 40% and fuel consumption can be reduced by up to 25%. However, under neither under-saturated condition nor over-saturated condition can this algorithm be efficient.

Furthermore, we take the market penetration rate (MPR) and the ASL implementation area into consideration. We find that our algorithm has little effect to system mobility when the MPR is very low; however, with the increasement of the MPR, the efficiency of our algorithm becomes increasingly apparent. The result of fuel consumption has the same pattern as that of system mobility, the efficiency of the algorithm improves with the increasement of the MPR. In addition, we find that when the ASL implementation area is too short, our algorithm cannot fully function; thus we propose a recommendation that ASL implementation area should be 100 to 150 meters,

so that the algorithm efficiency can be guaranteed and the computation cost will not be so high. Those results also conform to the principles of our algorithm.

As for the future study, we can extend our study from 3 aspects. Firstly, we can study how to make the algorithm work under over saturated condition; this may further help alleviate the traffic congestion. Secondly, we can apply our algorithm to more complicated systems, things like a system with turning behaviors. Finally, we can consider different categories of vehicles, things like buses and trucks, and explore what effect our algorithm will have on different types of vehicles.

Bibliography

environmental protection agency, U.S., . Sources of greenhouse gas emissions. https://www.epa.gov/ghgemissions/sources-greenhouse-gas-emissions#transportation. Accessed 2017.

Ahn, K., Rakha, H., 2008. The effects of route choice decisions on vehicle energy consumption and emissions. Transportation Research Part D: Transport and Environment 13, 151–167.

Ahn, K., Rakha, H., Trani, A., Van Aerde, M., 2002. Estimating vehicle fuel consumption and emissions based on instantaneous speed and acceleration levels. Journal of transportation engineering 128, 182–190.

Alam, M.S., McNabola, A., 2014. A critical review and assessment of eco-driving policy & technology: Benefits & limitations. Transport Policy 35, 42–49.

Apart, F., . Building america's future falling apart and falling .

Balakrishnan, G., Uppinakudru, G., Girwar Singh, G., Bangera, S., Dutt Raghavendra, A., Thangavel, D., 2014. A comparative study on visual choice reaction time for different colors in females. Neurology research international 2014.

Eckhoff, D., Halmos, B., German, R., 2013. Potentials and limitations of green light optimal speed advisory systems, in: 2013 IEEE Vehicular Networking Conference, IEEE. pp. 103–110.

Elliott, A.M., 2014. The future of the connected car. Mashab1e .

Elvik, R., 2012. Speed limits, enforcement, and health consequences. Annual review of public health 33, 225–238.

Geroliminis, N., Daganzo, C.F., 2008. Existence of urban-scale macroscopic fundamental diagrams: Some experimental findings. Transportation Research Part B: Methodological 42, 759–770.

He, X., Liu, H.X., Liu, X., 2015. Optimal vehicle speed trajectory on a signalized arterial with consideration of queue. Transportation Research Part C: Emerging Technologies 61, 106–120.

Hegyi, A., De Schutter, B., Hellendoorn, J., 2005. Optimal coordination of variable speed limits to suppress shock waves. IEEE Transactions on intelligent transportation systems 6, 102–112.

Huang, Y., Ng, E.C., Zhou, J.L., Surawski, N.C., Chan, E.F., Hong, G., 2018. Eco-driving technology for sustainable road transport: A review. Renewable and Sustainable Energy Reviews 93, 596–609.

Jalooli, A., Shaghaghi, E., Jabbarpour, M.R., Md Noor, R., Yeo, H., Jung, J.J., 2014. Intelligent advisory speed limit dedication in highway using vanet. The Scientific World Journal 2014.

Jin, W.L., Laval, J., 2018. Bounded acceleration traffic flow models: A unified approach. Transportation Research Part B: Methodological 111, 1–18.

Jin, W.L., Yu, Y., 2015a. Asymptotic solution and effective hamiltonian of a hamilton–jacobi equation in the modeling of traffic flow on a homogeneous signalized road. Journal de Mathématiques Pures et Appliquées 104, 982–1004.

Jin, W.L., Yu, Y., 2015b. Performance analysis and signal design for a stationary signalized ring road. arXiv preprint arXiv:1510.01216 .

Katsaros, K., Kernchen, R., Dianati, M., Rieck, D., 2011. Performance study of a green light optimized speed advisory (glosa) application using an integrated cooperative its simulation platform, in: 2011 7th International Wireless Communications and Mobile Computing Conference, IEEE. pp. 918–923.

Kesting, A., 2008. Microscopic modeling of human and automated driving: Towards traffic-adaptive cruise control .

Kesting, A., Treiber, M., Helbing, D., 2010. Enhanced intelligent driver model to access the impact of driving strategies on traffic capacity. Philosophical Transactions of the Royal Society A: Mathematical, Physical and Engineering Sciences 368, 4585–4605.

Killian, R., 2012. Ecodriving: The science and art of smarter driving. TR News .

Kwon, E., Brannan, D., Shouman, K., Isackson, C., Arseneau, B., 2007. Development and field evaluation of variable advisory speed limit system for work zones. Transportation research record 2015, 12–18.

Larsson, H., Ericsson, E., 2009. The effects of an acceleration advisory tool in vehicles for reduced fuel consumption and emissions. Transportation Research Part D: Transport and Environment 14, 141–146.

Li, S.E., Xu, S., Huang, X., Cheng, B., Peng, H., 2015. Eco-departure of connected vehicles with v2x communication at signalized intersections. IEEE Transactions on Vehicular Technology 64, 5439–5449.

Lighthill, M.J., Whitham, G.B., 1955. On kinematic waves ii. a theory of traffic flow on long crowded roads. Proceedings of the Royal Society of London. Series A. Mathematical and Physical Sciences 229, 317–345.

Luo, Y., Li, S., Zhang, S., Qin, Z., Li, K., 2017. Green light optimal speed advisory for hybrid electric vehicles. Mechanical Systems and Signal Processing 87, 30–44.

Mooney, C.Z., 1997. Monte carlo simulation. volume 116. Sage Publications.

Morales Fresquet, A., Jin, W.L., 2018. Evaluating the impacts of start-up and clearance behaviors in a signalized network: A network fundamental diagram approach .

Newell, G.F., 1961. Nonlinear effects in the dynamics of car following. Operations research 9, 209–229.

Newell, G.F., 2002. A simplified car-following theory: a lower order model. Transportation Research Part B: Methodological 36, 195–205.

Nissan, A., Koutsopoulosb, H.N., 2011. Evaluation of the impact of advisory variable speed limits on motorway capacity and level of service. Procedia-Social and Behavioral Sciences 16, 100–109.

Rakha, H., Ahn, K., Trani, A., 2003. Comparison of mobile5a, mobile6, vt-micro, and cmem models for estimating hot-stabilized light-duty gasoline vehicle emissions. Canadian Journal of Civil Engineering 30, 1010–1021.

Rakha, H., Kamalanathsharma, R.K., 2011. Eco-driving at signalized intersections using v2i communication, in: 2011 14th international IEEE conference on intelligent transportation systems (ITSC), IEEE. pp. 341–346.

Ranasinge, D.U., Jayanthi, W., Bunker, J.M., Bhaskar, A., 2017. Saturation headway variation at a signalised intersection approaches with a downstream bus stop and bicycle lane .

Roess, R., Prassas, E., McShane, W., 2011. Traffic engineering. 4th ed., Prentice Hall. Includes bibliographical references and index.

Strömberg, H., Karlsson, I.M., Rexfelt, O., 2015. Eco-driving: Drivers' understanding of the concept and implications for future interventions. Transport policy 39, 48–54.

Treiber, M., Hennecke, A., Helbing, D., 2000. Congested traffic states in empirical observations and microscopic simulations. Physical review E 62, 1805.

Ubiergo, G.A., Jin, W.L., 2016. Mobility and environment improvement of signalized networks through vehicle-to-infrastructure (v2i) communications. Transportation Research Part C: Emerging Technologies 68, 70–82.

Yang, H., Jin, W.L., 2014. A control theoretic formulation of green driving strategies based on inter-vehicle communications. Transportation Research Part C: Emerging Technologies 41, 48–60.

Yao, H., Cui, J., Li, X., Wang, Y., An, S., 2018. A trajectory smoothing method at signalized intersection based on individualized variable speed limits with location optimization. Transportation Research Part D: Transport and Environment 62, 456–473.

Zhang, Y., Fu, C., Hu, L., 2014. Yellow light dilemma zone researches: a review. Journal of traffic and transportation engineering (English edition) 1, 338–352.